**NURETH14-455** 

# INTERACTION EFFECTS BETWEEN LAMINAR NATURAL CONVECTION AND SURFACE THERMAL RADIATION IN PHWR REACTOR CHANNELS

Deepthi Chandramouli<sup>1</sup>, M. Rajendrakumar<sup>2</sup>, K. Velusamy<sup>2</sup> and P.Chellapandi<sup>2</sup>

<sup>1</sup>National Institute of Technology, Trichy, India

<sup>2</sup>Indira Gandhi Centre for Atomic Research, Kalpakkam, India

deepthi1223@gmail.com, mrk@igcar.gov.in

### **Abstract**

Pressurized Heavy Water Reactor (PHWR) reactor channel consists of a pressure tube (PT), which is concentrically placed inside the calendria tube (CT). After a hypothetical loss of coolant accident, sagging or ballooning of the PT may occur and physical contact between PT and CT takes place. Under this condition, knowledge of temperature distributions in PT and CT are essential to assess their structural integrity. Towards this, a 2-D CFD study has been carried out to understand the natural convection of CO<sub>2</sub> and surface thermal radiation. Detailed parametric study has been carried for various values of temperature difference, emissivity and eccentricity.

### Introduction

India's current nuclear power program is based on the Pressurized Heavy Water Reactor (PHWR), with a large number of reactors in operation and many under construction. The PHWRs consist of a horizontal reactor core with a large number of parallel reactor channels. The entire reactor channels are submerged in a pool of heavy water (moderator), maintained at 65°C. Each channel consists of a pressure tube (PT), which is concentrically placed inside the calendria tube (CT). The space between the tubes is filled with carbon dioxide gas for thermal insulation and also to prevent any oxidation of tubes. During a hypothetical loss of coolant accident along with the failure of the emergency cores cooling system, the temperature of the PT increases. This increase in temperature leads to deterioration of structural properties which in turn leads to either sagging or ballooning of the PT. This sagging or ballooning leads to a physical contact between the PT and CT and when the PT touches the calendria tube, temperature inside PT decreases because of increase in heat transfer to moderator. It is an important aspect in reactor safety to study the behavior of PT in order to assess its structural integrity during this process. This assessment requires detailed knowledge of heat transfer characteristics between PT and CT, by natural convection of CO2 and surface thermal radiation. The complete PT-CT assembly can be simplified as a cylindrical annulus by neglecting the heat transfer in the axial directions because of the loss of coolant flow.

The present work deals with the investigation of the laminar natural convection heat transfer combined with the effects of surface radiation in both concentric and eccentric cylindrical annulus configurations. Cases dealing with pure laminar natural convection are being studied extensively, but the effects of thermal radiation and conduction through walls of the cylinders

have been overlooked in most of these cases. When the effects of radiation are also considered, natural convection gets suppressed, i.e., the surface radiation tends to decrease the heat flux associated with convection. The effect of emissivity, temperature difference and eccentricity on the overall Nusselt number is the main objective of the present study. Further, the technological applications extends to underground transmission cables, heat transfer in nuclear reactors, cooling of electrical and electronic components, solar heat collection using concentrators, heat removal from gas-cooled fast reactors, design of high-temperature heat exchangers, etc.

A comprehensive review of the literature on the analyses of natural convection and radiative heat transfer in cylindrical annulus will provide a clear picture of all the possible applications till date, improvements and limitations of the numerical and experimental investigations and the scope for future study. Kuehn and Goldstein [1] conducted experimental as well as numerical simulations for investigating natural convection between two concentric cylinders, where gap was filled with air or water. They determined local equivalent conductivities for both inner and outer cylinders for different Rayleigh numbers. They also studied the influence of diameter ratio and Prandtl number in the low Rayleigh number regime. Kuehn and Goldstein [2] derived relations for Nusselt number for natural convection heat transfer in horizontal concentric cylinders. Kuehn and Goldstein [3] established a correlation for Nusselt number as a function of Rayleigh number for concentric and eccentric cases where cylinder outer wall is subjected to an isothermal boundary condition. They established the variation of conduction Nusselt number within an enclosure with eccentricity. They also formulated methods to calculate the overall Nusselt number and equivalent thermal conductivities from the inner and outer surface Nusselt number and conduction Nusselt number.

Pepper and Cooper [4] studied natural convection flow in the eccentric annular space between two isothermal cylinders. A decrease in the inner Nusselt number occurs when the inner cylinder is moved towards the upper region of the outer cylinder; accordingly the outer Nusselt number increases. Guj and Stella [5] investigated the effect of eccentricity on the Nusselt number and found that Nusselt number was almost insensitive to the effect of horizontal eccentricity, in the absence of surface radiation. Sambamurthy et al. [6] studied laminar conjugate natural convection in horizontal annuli and developed correlations for Nusselt number as functions of Grashof number for different configurations, aspect ratios and thermal conductivity ratios. Studies considering the effect of surface radiation are however, fewer in number. Natural convection in concentric and eccentric annuli with mixed boundary conditions was discussed by Ho and Lin [7]. It was found that Nusselt number increased with modified Rayleigh number and they also formulated a correlation between Nusselt number and Rayleigh number for typical eccentricities. The first numerical study of the coupled heat transfer problem involving both convection and radiation in a rectangular cavity seems to be that of Larson and Viskanta [8]. They found that radiation heats up the cavity surface and the gas body very quickly and thus considerably modifies the flow pattern and the corresponding convection process. Shaija et al. [9] performed studies on effect of surface radiation on conjugate natural convection in a horizontal annulus driven by inner heat generating solid cylinder. They concluded that convective Nusselt number reduces with increasing emissivity values of the surfaces whereas radiative Nusselt number increases with the same.

# 1. Mathematical modelling and Problem Formulation

The 220 MWe PHWRs consist of a horizontal reactor core of 306 parallel reactor channels. The coolant flows through half of the channels in one direction and in the remaining channels in the opposite direction [10]. Each reactor channel consists of a PT of 90 mm outside diameter and 3.8 mm thickness, which is concentrically placed in a CT of 110 mm outside diameter and 1.5 mm thickness (Fig. 1).

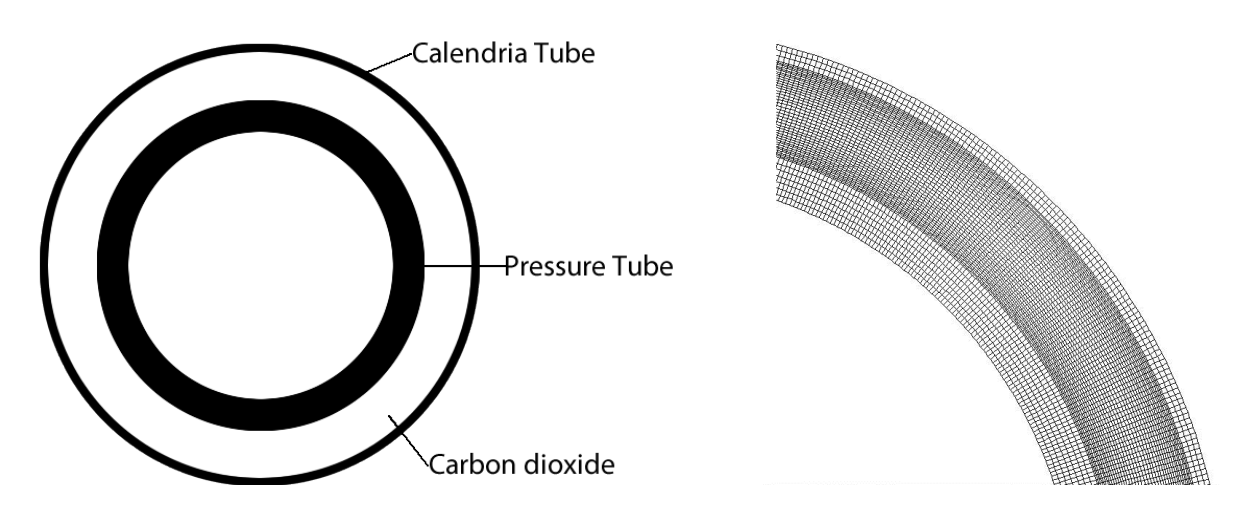


Figure 1 Schematic model of PT-CT geometry under consideration.

Figure 2 Computational Mesh of PT-CT assemblies

The PT and the CT are made of Zirconium 2.5 wt % Nb and Zircaloy-2 material respectively. The meshed cavity for the geometry is shown in the Fig. 2. The size of the mesh chosen for the simulation was 500x200. The element chosen is of quad type and mesh near the wall is made fine to account for the high velocity gradient regime.

## 1.1 Governing Equations for fluid flow and Radiative heat transfer

The equations that govern the CO2 flow and heat transfer processes in the annulus are:

Continuity:

$$\frac{\partial}{\partial x_i} \left( \rho u_j \right) = 0 \tag{1}$$

Momentum:

$$\frac{\partial}{\partial x_j} \left( \rho u_j u_i - \mu \frac{\partial u_i}{\partial x_j} \right) = -\frac{\partial p}{\partial x_i}$$
 (2)

Energy:

$$\frac{\partial}{\partial x_{i}} \left( \rho u_{j} c_{p} T - K \frac{\partial T}{\partial x_{i}} \right) = 0 \tag{5}$$

Surface to surface radiation modeling of heat transfer is based on tracking beams via the DTRM [11]. An inbuilt algorithm is used for calculating view factors between patches from the CFD volume mesh. The view factor  $F_{ij}$  between patches i and j is the fraction of the total radiation

leaving surface i that is incident on surface j. In the present treatment, the incident radiation is taken to be contained in all beams from i striking j, i.e.

$$F_{ij} = \sum_{k=1}^{N_{L,i}} \alpha_k f_{ij} \tag{6}$$

where  $f_{ij}$  is the view factor for a single beam.

The total radiation flux J<sub>i</sub> leaving patch is given by

$$J_i = \varepsilon \ E_{B,i} + \rho_r I_i \tag{7}$$

Where  $I_i$  is the total incident radiation flux from other patches onto patch i. The incident flux  $I_i$  is expressed in terms of the radiosities of all the other patches.

$$I_i = \sum_{i} F_{ji} J_j \tag{8}$$

The net radiant heat flux at the wall patch i,  $q_r$ , is given by the difference between the arriving and leaving fluxes,

$$q_r'' = I_i - J_i = \alpha_r I - \varepsilon E_B \tag{9}$$

# 1.2 Boundary Conditions and Solution Procedure

The inner surface of pressure tube is kept constant at either 573 or 953 K [10]. The Rayleigh number for both the cases is 2000 and 3000 respectively. The outer surface of Calendria tube is subjected to convection boundary condition with 200 W/m²K as the convective heat transfer coefficient and 338 K as the fluid temperature. The natural convection of CO2 is modeled by the Boussinesq approximation. The flow and temperature distributions have been solved as a conjugate problem by the general-purpose thermal hydraulics code Star-CD [11]. This code uses Finite Volume Method for solving governing equations. The pressure-velocity coupling in the flow equations is resolved using the SIMPLE algorithm [12].

## 2. Validation and Mesh Independency Study

## 2.1 Validation

The CFD code and the solution methodology used in the present work are validated by simulating a number of benchmarking problems. The results obtained in the present study are then compared with those available in the literature. Natural convective flow in a differentially heated concentric annulus is simulated and the results are compared with those of Kuehn and Goldstein [1 and 2]. Simulation is carried out for a Prandtl Number of 0.71, radius ratio of 2.6, L/Di of 0.8. Kuehn and Goldstein reported equivalent thermal conductivities for inner and outer wall for different Rayleigh Number and Nusselt Number is calculated from these equivalent thermal conductivities and compared with the present work. Table 1 shows the comparison of present results with those of Kuehn and Goldstein [1] for a concentric annulus and a good agreement with results of Kuehn and Goldstein [1] is observed. Further, it can be seen that there is no difference between the inner and outer surface Nusselt Number compared to the small difference predicted by Kuehn and Goldstein [1]. Kuehn and Goldstein [2] obtained equations for natural convection heat transfer using a conduction boundary-layer model. Table 1 shows the

comparison of present results with those of Kuehn and Goldstein [2] for a concentric annulus case. The number in the braces represents the deviation of present result from those of Kuehn and Goldstein [2] and it is clear that the difference decreases drastically with increasing Rayleigh Number.

	Nusselt Number							
Rayleigh Number	Present Work			Kueh Goldst Theor	ein [1]	Kuehn and Goldstein [1] Experimental	[2] Kuehn and Goldstein [2]	
	Inner	Outer	Average	Inner	Outer	Average	Average	
$1 \times 10^{3}$	2.28	2.28	2.28	2.26	2.27	NA	2.92 (28%)	
$1 \times 10^4$	4.18	4.18	4.18	4.21	4.20	NA	4.64 (11%)	
$2.5 \times 10^4$	5.31	5.31	5.31	5.30	5.40	5.25	5.65 (6%)	
$5 \times 10^4$	6.26	6.26	6.26	6.33	6.22	6.33	6.59 (5%)	
$1 \times 10^{5}$	7 35	7 35	7 35	NA	NA	NA	7 70 (4%)	

Table 2 Comparison of Nusselt Number with those of Kuehn and Goldstein [1 & 2]

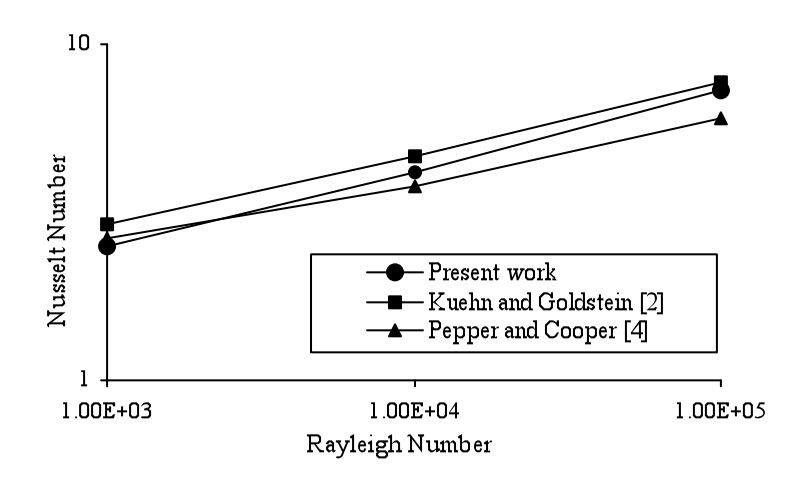


Figure 3 Comparison of Nusselt Number for eccentric horizontal cylindrical annulus with literature

Further, simulations have been carried out for an eccentric annulus and the results are compared with those of Pepper and Cooper [4] and with correlations formulated by Kuehn and Goldstein [3] and shown in Fig. 3. Simulations were carried out for a Prandtl Number of 0.7, radius ratio of 2.6, L/Di of 0.8 and eccentricity of -0.325. It is found that the numerically computed Nusselt Number in the present work matches up with the reported data by 10%. Though the difference is more, it is evident from Fig. 3 that the present results lie in between the reported values. As the last part of the validation exercises, natural convection and radiation heat transfer in cylindrical annulus is simulated and the results are used to validate the radiation models used in the present study. Shaija and Narasimham [9] investigated the interaction of surface radiation with natural convection. In the present work, the exact problem is simulated and maximum temperature of the

inner solid cylinder is computed. The simulation is carried out with outer cylinder maintained at 300K, radius ratio at 0.452, ratio of thermal conductivities of inner cylinder & fluid at 5. The surface emissivity and the inner cylinder heat generation are varied and computed temperatures are shown in Table 2. Maximum temperature matches well with those of Shaija and Narasimham [9] at lower emissivities and this difference increases at rapid rate with increase in emissivity and Grashof Number.

Emissivity	0.0	0.4	0.6
T <sub>max</sub> (K) (present Work)	322.7	319	317.6
T <sub>max</sub> (K) [shaija et al (2009)]	322.9	315.7	313.4

Table 2 Comparison of Nusselt Number with those of [9]

# 2.2 Grid Independence Study

The grid independency study of the solution was carried for two different meshes i.e., one with concentric cylinders with  $T_h = 953$  K,  $\epsilon = 0.0$  and the other one with eccentric cylinders with  $\xi = 0.99$  in the downward direction,  $T_h = 573$  K,  $\epsilon = 0.4$ . Three different grid sizes were used for the grid independent study. The heat transfer coefficient is calculated at the hot wall. Table 3 shows the average Nusselt number for the first case. Results show that a maximum of 1% difference is observed in the Nusselt number between the meshes which indicates that a mesh independent solution is obtained and a mesh with 30720 cells is selected for further simulation. Table 4 shows the values of Nusselt number for different mesh sizes for the second case. Results show that a maximum of 1% difference is observed in the Nusselt number between the meshes which indicates that a mesh independent solution is obtained and a mesh with 24628 cells is selected for further simulation

Number of cells	Average Nusselt Number				
7680	19.03				
30720	19.14				
122880	19.15				

Table 3 Nusselt number for various mesh
sizes ( $\xi = 0.0$ , $T_h = 953$ K, $\epsilon = 0.0$ )

Number of Cells	Average Nusselt Number				
6157	72.21				
24628	72.49				
98512	72.87				

Table 4 Nusselt number for various mesh sizes  $(\xi = 0.99, T_h = 573 \text{ K}, \varepsilon = 0.4)$ 

## 3. Results and Discussions

Simulations were carried out by varying emissivity in the range 0-0.99 and eccentricity in the upward, downward and right hand side directions in the range of 0-0.9. Comparisons are made, based on the stream function and isotherm contours as well as average Nusselt number. In these discussions, Nusselt number was calculated from  $Nu = hD_i/k$ , where heat transfer coefficient (h) is calculated from,  $h = Q/(\Delta T)^*(\pi D_i L_c)$ .

## 3.1 Contours and Streamlines

Streamlines and temperature contours for different eccentricity directions and positions are shown in Figs. 4 - 6. In all the three cases, the temperature of the outer wall, its variation is least

when the inner cylinder is concentric and is maximum when the inner cylinder almost touches the outer one. Also, the average value of temperature of the outer wall is maximum when the inner cylinder almost touches the outer cylinder.

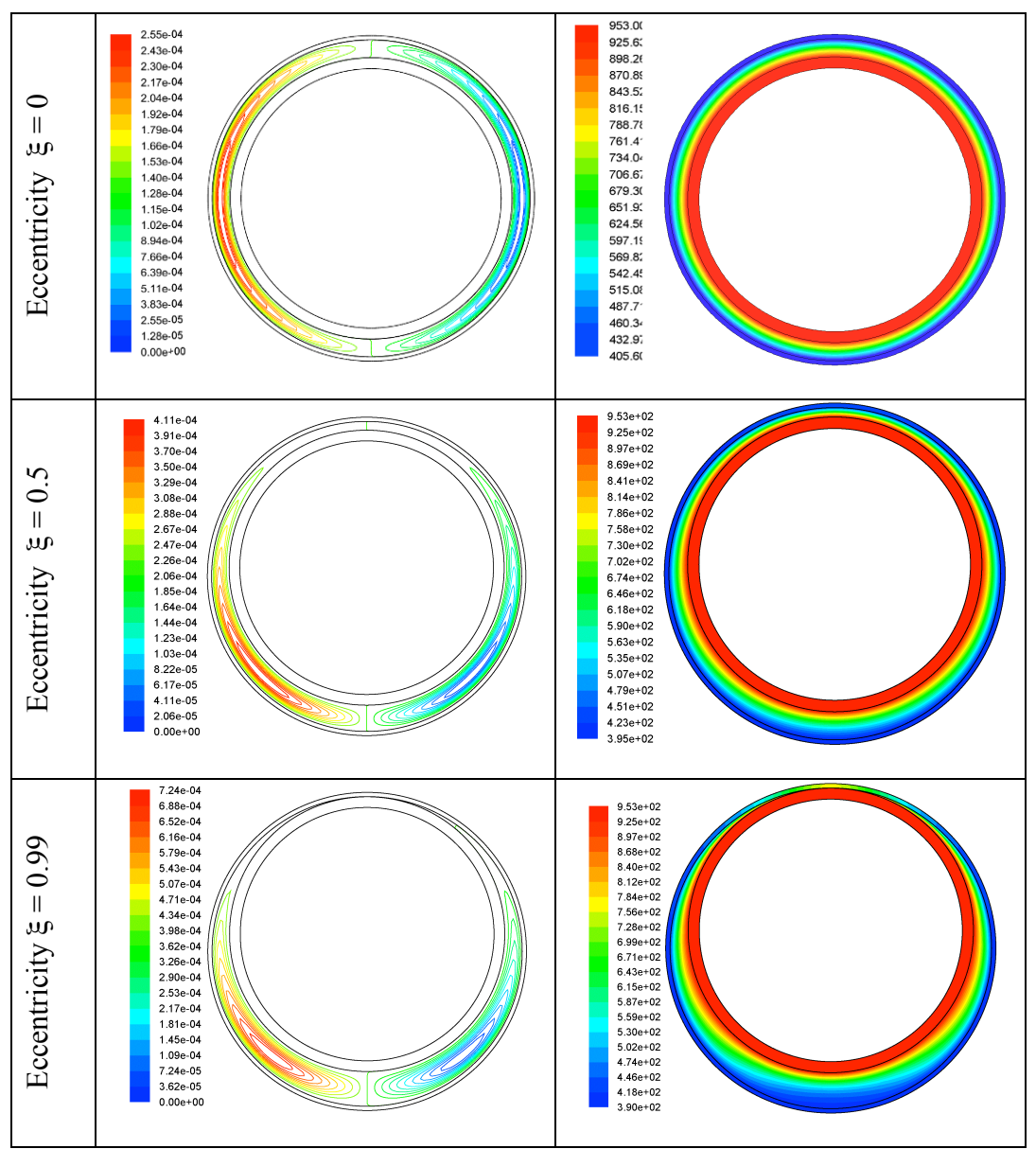


Figure 4 Streamlines and Velocity contours for different eccentricities in the upward direction ( $T_h$  = 953 K ,  $\epsilon$  = 0.4)

Figure 4 shows the case when the inner cylinder is displaced eccentrically upwards. From the streamlines, it is clear that the eye of the streamlines moves downwards when the inner cylinder is moved upwards. The maximum stream function value also increases when inner cylinder is moved upwards. This is due to reduction in the flow resistance as a consequence of increase in gap width at the bottom. From the temperature contours, it can be seen that both inner cylinder and outer cylinder has their own thermal boundary layer in the concentric position. When the

inner cylinder is moved upwards, the thermal boundary layer of the outer cylinder increases at the bottom and reaches a maximum when inner cylinder touches the outer cylinder at the top.

Figure 5 shows the case when the inner cylinder is displaced eccentrically downwards. Both, streamlines as well as isotherms are symmetric with respect to the vertical axis. From the streamlines, it is clear that the eye of the streamlines moves upwards when the inner cylinder is moved downwards. The maximum stream function values also increases when inner cylinder is moved downwards. Since the aspect ratio of the present configuration is nearly 1, no visible difference is observed in the profile of streamlines and temperature contours, as the flow features in these annuli are controlled more by flow resistance than by buoyancy.

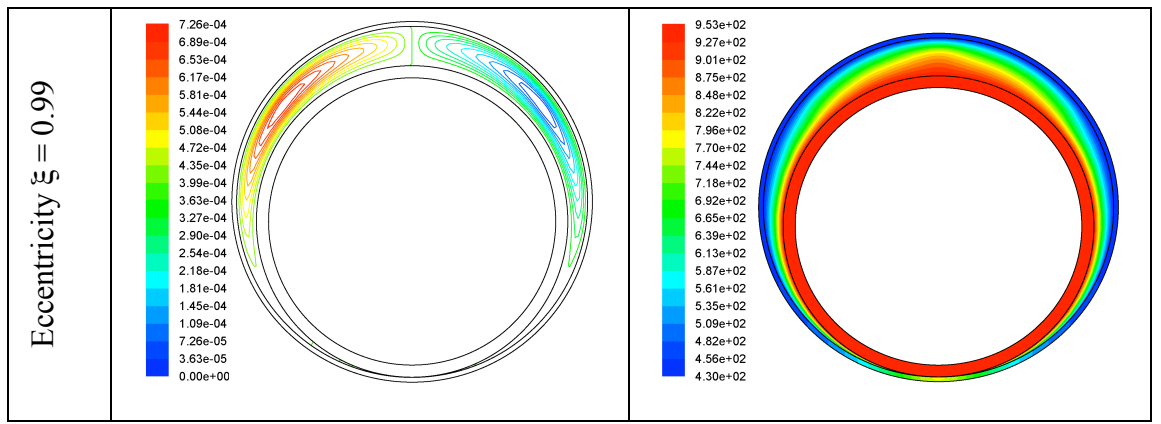


Figure 5 Streamlines and Velocity contours for different eccentricities in the downward direction  $(T_h = 953 \text{ K}, \epsilon = 0.4)$ 

Figure 6 shows the isotherms and streamlines for cases when the inner cylinder in displaced in the right hand side direction. It is clear that the isotherms and the streamlines are not symmetrical, but are shifted to the right. The extent to which they are shifted depends upon the extent of eccentricity.

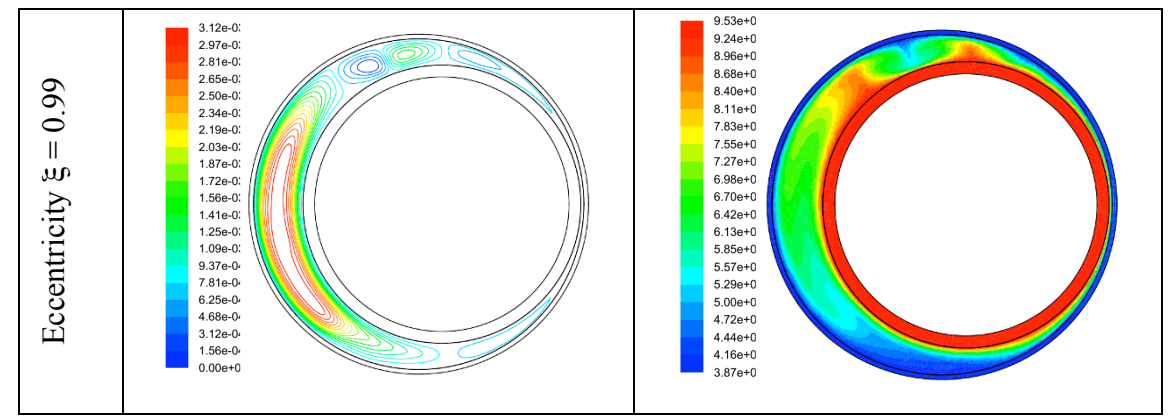


Figure 6 Streamlines and Velocity contours for different eccentricities in the rightward direction ( $T_h = 953 \text{ K}, \epsilon = 0.4$ )

The main streamline loop splits into three loop (one bigger loop and 2 smaller loops) when the inner cylinder touches the outer cylinder and similar distortion is observed in the temperature

contours also. As a result of this, non-monotonic temperature distribution develops on the outer cylinder which is in contact with the moderator.

# 3.2 Effect of Eccentricity

Figures 7 shows the variation of the Nusselt number when eccentricity,  $\xi$  changes from 0 to 0.99 with  $T_h = 953$  K and  $\epsilon = 0.0$ . Because of difficulty in meshing, simulation for the case when eccentricity is 1 is not considered. The change in Nusselt number is minimum when the inner cylinder is eccentrically moved in the rightward direction and is maximum when the inner cylinder is eccentrically moved in upward or downward direction. It can seen that for upward or downward movement of the PT, the Nusselt number reaches a minimum at an eccentricity of  $\sim 0.25$ . This minimum value is about 50% of the concentric cylinder value. However, the eccentricity increases further, the Nusselt number increases to over 3 times that of the concentric cylinder value. This is due to dominance of conduction heat transfer in CO2 at high eccentricity values. In the case of horizontal eccentricity, similar minimum occurs at a larger value of eccentricity.

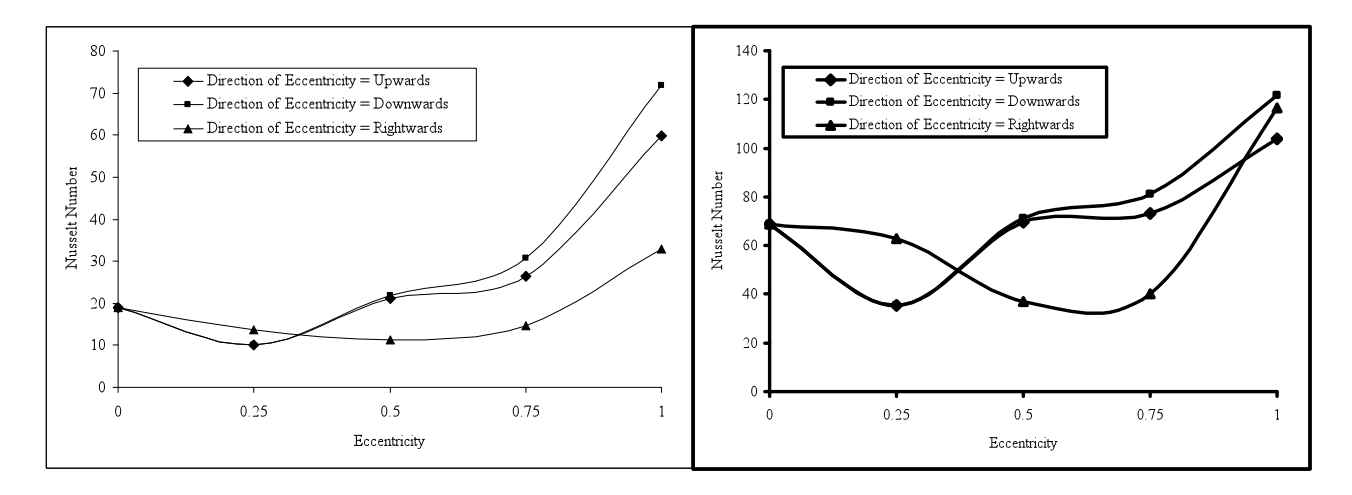


Figure 7 Variation of Nusselt Number with eccentricity  $\xi$  for different Eccentricity directions  $(T_h = 953~K~,~\epsilon = 0.0)$ 

Figure 8 Variation of Nusselt Number with eccentricity  $\xi$  for different Eccentricity directions (T<sub>h</sub> = 953 K,  $\epsilon$  = 0.4)

Figure 8 shows the variation of the Nusselt number when eccentricity,  $\xi$  changes from 0 to 0.99 with  $T_h$  at 953 K and  $\epsilon=0.4$ . From Figs. 7 and 8, it is clear that the dependence of Nusselt number on eccentricity is nearly similar, with Nusselt number value being higher at higher emissivity. This increase can be attributed to the increased total heat transfer rate or decreased convective heat transfer rate because of addition of radiative heat transfer. Because of radiation, the inner and outer wall temperatures tend to become uniform leading to increased Nusselt number. Figures 9 and 10 show the variation of Nusselt number when eccentricity,  $\xi$  changes from 0 to 0.99 with  $\epsilon=0.4$  for two values  $T_h$ , viz., 573K and 953K. It is clear that Nusselt number increases when the  $T_h$  or in other words Rayleigh number increases. From Figs. 9 and

10, it is evident that variation in Nusselt number is increasingly non-uniform with increase in Rayleigh number.

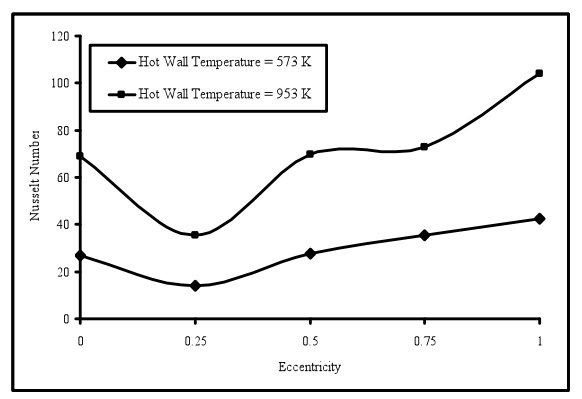


Figure 9 Variation of Nusselt Number with eccentricity  $\xi$  for different inner wall temperatures ( $\epsilon = 0.4$ , Eccentricity Direction = Upward)

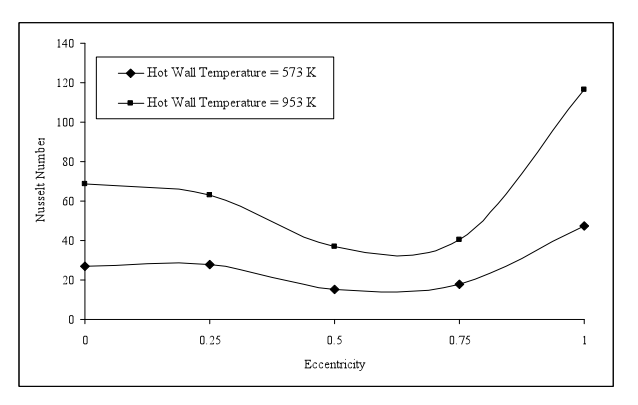


Figure 10 Variation of Nusselt Number with eccentricity  $\xi$  for different inner wall temperatures ( $\epsilon = 0.4$ , Eccentricity Direction = Rightward)

# 3.3 Effect of Emissivity

Figures 11 and 12 show the effect of emissivity on Nusselt Number for upward and rightward eccentricities for  $T_h = 573 K$  and Figs 13 and 14 show the effect of emissivity on Nusselt Number for upward and rightward eccentricities for  $T_h = 953 K$ . The Nusselt number increases monotonically with increase in the emissivity as expected.

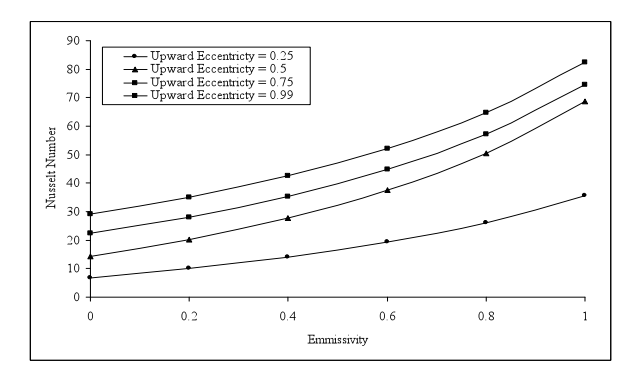


Figure 11 Variation of Nusselt Number with emissivity for different  $\xi$  ( $T_h = 573~K$ , Eccentricity Direction = Upward)

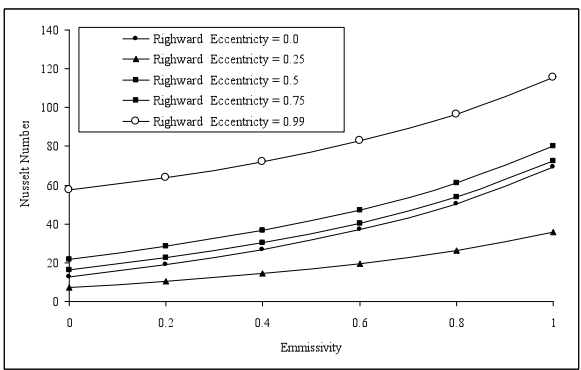


Figure 12 Variation of Nusselt Number with emissivity for different  $\xi$  ( $T_h = 573 \text{ K}$ , Eccentricity Direction = Rightward)

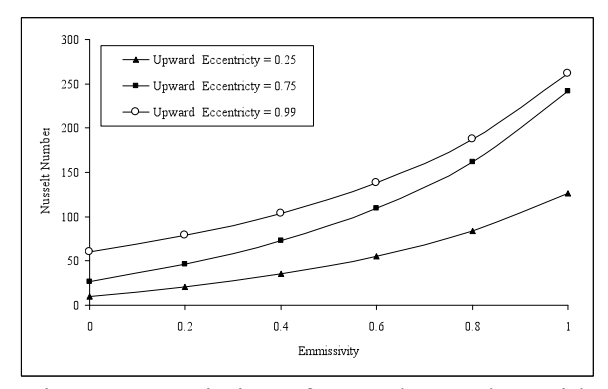


Figure 13 Variation of Nusselt Number with emissivity for different  $\xi$  ( $T_h = 953 \text{ K}$ , Eccentricity Direction = Upward)

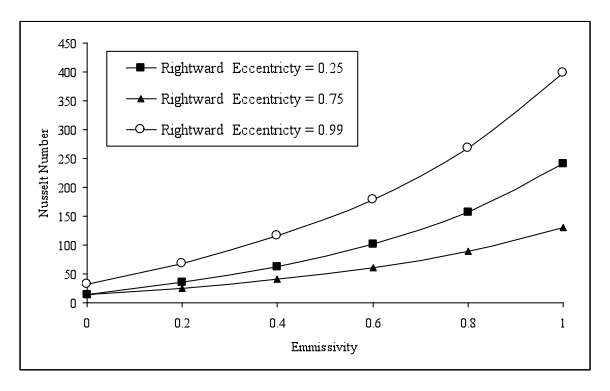


Figure 14 Variation of Nusselt Number with emissivity for different  $\xi$  ( $T_h = 953 \text{ K}$ , Eccentricity Direction = Rightward)

### 4. Conclusions

Conjugate laminar natural convection, conduction and radiative heat transfer through CO2 gas in the annular gap between PT and CT has been investigated. Detailed parametric studies, varying the PT temperature, emissivity of tube surfaces and eccentricity as a result of sagging of the PT have been carried out. Engineering results of Nusselt number as a function of various parameters are obtained. It is seen that the Nusselt number approaches a minimum when eccentricity increases from zero. This minimum is about 50% of that at concentric orientation. As the eccentricity increases further, the Nusselt number increases due to dominance of conduction heat transfer. As the Rayleigh number increases, variation in Nusselt number becomes increasingly non-uniform. Also, the Nusselt number monotonically increases with emissivity. These Nusselt number values are useful for the thermal mechanical analysis of PT and CT.

## 5. Nomenclature

α	Thermal Diffusivity of heat $(k/\rho C_p)$		L	Characteristic Length, (D <sub>0</sub> – D <sub>i</sub> )/2	
$\alpha_{\scriptscriptstyle k}$	Surface Absorptivity		L <sub>c</sub>	Length of the cylinders (assumed to be 1m)	
β	Thermal Coefficient of expansion(K <sup>-1</sup> )		N	No. of Radiation Surfaces	
$C_{\mathfrak{p}}$	Specific heat capacity (J/Kg/K		Nu	Nusselt number ( $Nu = hD_i/k$ )	
ΔΤ	Temperature difference between hot wall and fluid temperature (K)		p	Pizeometric pressure = $p_s$ - $\rho_0 gx$	
$D_{i}$	Outside Diameter of Pressure Tube, m		ps	Static pressure	
Do	Inside Diameter of Calendria Tube, m		ρ	Density	
De	Distance between centers of PT at original and eccentrically moved position, m		$\rho_0$	Reference density	
$E_{B,i}$	Black body emission flux (W/m <sup>2)</sup>		$ ho_r$	Reflectivity	
3	Surface Emissivity		Q	Total heat transfer (W)	
ξ	Non-dimensional Eccentricity (De / Li)		Ra	Rayleigh Number (gβΔTL/vα)	
fij	View factor for a single beam emanating from the given cell		Т	Temperature (K)	

Fij	View factor between patches <i>i</i> and <i>j</i>	$T_h$	Hot wall Temperature (K)
g	Acceleration due to gravity	$T_0$	Reference temperature (K)
Gr	Grashof Number $(g\beta\Delta TL/v^2)$ )	ui	Velocity component in direction x <sub>i</sub>
h	Overall heat transfer co-efficient (W/m <sup>2</sup> K)	$u_i$	Velocity component in direction x <sub>i</sub>
Ii	Total incident radiation flux (W/m <sup>2</sup> )	μ	molecular dynamic fluid viscosity
Ji	Total Radiation flux (W/m <sup>2</sup> )	Xi	Cartesian coordinate (i =1,2,3)
k	Thermal conductivity of the fluid (W/mK)	Xi	Cartesian coordinate $(j = 1,2,3)$

## 6. References

- [1]. T.H. Kuehn and R.J. Goldstein, "An Experimental and Theoretical Study of Natural Convection in the Annulus between Horizontal Concentric Cylinders", J. Fluid Mech., Vol. 74, 1976, pp. 695-719.
- [2]. T.H. Kuehn and R.J. Goldstein, "Correlating Equations for Natural Convection Heat Transfer between Horizontal Circular Cylinders", Int. J. Heat Mass Transfer, Vol. 19, 1976, pp. 1127-1134.
- [3]. T.H. Kuehn and R.J. Goldstein, "An Experimental Study of Natural Convection Heat Transfer in Concentric and Eccentric Horizontal Cylindrical Annuli", J. Heat Transfer ASME, Vol. 100, 1978, 635-640.
- [4]. D. W. Pepper and R. E. Cooper, "Numerical Solution of Natural Convection in Eccentric Annuli," AIAA J., Vol. 21, No. 9, 1983, pp. 1331-1337.
- [5]. G. Guj and F. Stella, "Natural Convection in Horizontal Eccentric Annuli: Numerical Study," Numerical Heat Transfer, Part A, Vol. 27, 1995, pp. 89-105.
- [6]. N.B. Sambamurthya, A. Shaijaa, G.S.V.L. Narasimham and M.V. Krishna Murthy, "Laminar conjugate natural convection in horizontal annuli", International Journal of Heat and Fluid Flow, Vol. 29, Issue 5, 2008, pp. 1347-1359.
- [7]. C. J. Ho and Y. H. Lin, "Thermal convection heat transfer of air/water layers enclosed in horizontal annuli with mixed boundary conditions", Heat and Mass Transfer, Vol. 24, Issue. 4, 1988, pp. 211-224.
- [8]. D.W. Larson and R. Viskanta, "Transient combined laminar free convection and radiation in a rectangular enclosure", J. Fluid Mech., Vol. 78, 1976, pp. 65–85.
- [9]. A. Shaija and G.S.V.L. Narasimham, "Effect of Surface Radiation on Conjugate Natural Convection in a Horizontal Annulus Driven by Inner Heat Generating Solid Cylinder", International Journal of Heat and Mass Transfer, Vol. 52, 2009, pp. 5759-5769.
- [10]. Ravi Kumar, Gopal Nandan, P. K. Sahoo, B. Chatterjee, D. Mukhopadhyay, H. G. Lele, "Ballooning of pressure tube under LOCA in an Indian Pressurized Heavy Water Reactor" <u>Proceedings of the International Heat Transfer Conference</u>, Washington, DC, USA, August 8-13, 2010,
- [11]. CD adapco Group, STAR-CD, ver. 3.2, Computational Dynamics Limited, 2005
- [12]. S. V. Patankar and D. B. Spalding, "A calculation procedure for heat, mass and momentum transfer in three-dimensional parabolic flows", International Journal of Heat and Mass Transfer, V 15, Issue 10, 1972.